FOI-R--0941--SE
December 2003
ISSN 1650-1942
Scientific report

Array Mapping for the SESAM System: Optimal Transformation Matrix Design

Per Hyberg

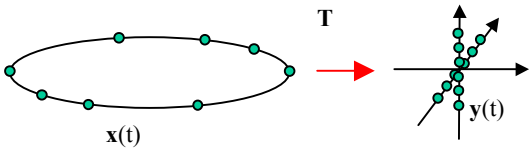

Command and Control Systems
SE-581 11 Linköping, Sweden

SWEDISH DEFENCE RESEARCH AGENCY

Command and Control Systems
P.O. Box 1165
SE-581 11 Linköping, Sweden

FOI-R--0941--SE

December 2003

ISSN 1650-1942

Scientific report

Array Mapping for the SESAM System: Optimal Transformation Matrix Design

Per Hyberg

Issuing organization	Report number, ISRN	Report type
FOI – Swedish Defence Research Agency Command and Control Systems P.O. Box 1165 SE-581 11 Linköping, Sweden	FOI-R--0941--SE	Scientific report
	Research area code Defence funded research	
	Month year December 2003	**Project no.** E 7059
	Customers code 6. Electronic Warfare	
	Sub area code 61 Electronic Warfare and HPM	

Author/s (editor/s)	Project manager
Per Hyberg FOI 18	Stefan Ahlgren
	Approved by Martin Rantzer
	Sponsoring agency The Swedish Armed Forces
	Scientifically and technically responsible Per Hyberg

Report title

Array Mapping for the SESAM System: Optimal Transformation Matrix Design

Abstract (not more than 200 words)

Mapping of the data output vector from an existing antenna array onto the data vector of an imaginary array of more suitable configuration is well known in array signal processing. By mapping onto an array manifold of lower dimension or uniform structure f. ex., processing speed can be improved. Conditions for the retaining of DOA estimate variance under such mapping have been formulated by several authors but the equally important systematic mapping errors, *the bias*, has been less treated to date.

This paper uses a geometrical interpretation of a Taylor expansion of the DOA estimator cost function to derive an alternative design of the mapping matrix that almost completely removes the bias. The key feature of the proposed design is that it takes the orthogonality between the manifold mapping errors and certain gradients of the estimator cost function into account.

Verifying simulations are given which show that mapping bias can be reduced by a factor of 100 or more especially in difficult situations involving a near ambiguous real array. A multi step procedure is proposed which in addition gives optimal variance performance.

Keywords

Bias minimization, array signal processing, direction finding, circular arrays

Further bibliographic information	Language English
ISSN 1650-1942	**Pages** 16 p.
	Price acc. to pricelist

Utgivare	Rapportnummer, ISRN	Klassificering
Totalförsvarets Forskningsinstitut - FOI	FOI-R--0941--SE	Vetenskaplig rapport
Ledningssystem	**Forskningsområde**	
Box 1165	6. Telekrig	
581 11 Linköping	**Månad, år**	**Projektnummer**
	December 2003	E 7059
	Verksamhetsgren	
	Forskning för FM	
	Delområde	
	61. Telekrig inklusive HPM	

Författare/redaktör	Projektledare
Per Hyberg FOI 18	Stefan Ahlgren
	Godkänd av
	Martin Rantzer
	Uppdragsgivare/kundbeteckning
	FM
	Tekniskt och/eller vetenskapligt ansvarig
	Per Hyberg

Rapportens titel (i översättning)

Array-mappning för SESAM-systemet: Design av optimala transformationsmatriser

Sammanfattning (högst 200 ord)

Avbildning (mappning) av utdatavektorerna från en existerande antenn-array på motsvarande utdatavektorer från en virtuell antenn-array är en välkänd procedur. Fördelen är att array-egenskaperna och bärings (DOA) -beräkningen kan optimeras separat, exempelvis kan man kombinera snabba beräkningsalgoritmer avsedda för raka linjära array:er med runtomtäckning, d.v.s. cirkulära array:er. Villkor för att bevara mätnoggrannheten (bäringsestimatens *varians*) under sådan avbildning har formulerats av flera författare men hittills har de systematiska bäringsfelen ("*bias*") behandlats i betydligt mindre omfattning. I rapporten visas att dessa senare fel kan dominera, speciellt i signalspaningsscenarier med krav på stor bandbredd.

Föreliggande rapport utnyttjar en geometrisk tolkning av en Taylorutveckling av DOA-estimatorns kostnadsfunktion för att härleda en algoritm varmed transformationsmatriser **T** kan konstrueras som nästan helt elliminerar ovan nämnda bias. Nyckeln ligger i att konstruera **T** så att avbildningsfelen blir ortogonala mot vissa av kostnadsfunktionens gradienter.

Verifierande simuleringar redovisas där de systematiska felen reducerats upp till 100 gånger trots att den runda array:en haft ett elementavstånd av 4 våglängder. En flerstegsprocedur föreslås också varmed även variansen hos bäringsestimaten kan minimeras.

Nyckelord

Bias-minimering, gruppantenner, riktningsestimering, kortvågspejling

Övriga bibliografiska uppgifter	Språk Engelska
ISSN 1650-1942	**Antal sidor:** 16 s.
Distribution enligt missiv	**Pris: Enligt prislista**

Contents

Array Mapping:
Optimal Transformation Matrix Design

Per Hyberg

I. INTRODUCTION

The concept of array mapping was introduced around 1990 by Friedlander [1], and Weiss & Friedlander [6], who in several papers suggested and analyzed different applications such as interpolation between calibrated directions, spatial smoothing, a. s. o. An application studied also by many other authors, Eriksson & Viberg, [8], Eriksson [13], is mapping from non-uniform wide spaced linear arrays, NULA:s, onto $\lambda/2$ spaced ULA:s in order to allow the faster rooting estimators and still keep the superior resolution or bandwidth of the larger non-uniform array. Furthermore, the performance of mapped root-MUSIC and MODE has been studied in several papers 1990-1995, Friedlander [4] and Weiss, Friedlander & Stoica [7].

One way of speeding up the DOA estimation process is *manifold dimension reduction* by mapping the real array onto a similar imaginary array with fewer elements. This type of mapping, including conditions to preserve DOA accuracy, has been treated in Andersson [3], Eriksson & Viberg, [8] and Eriksson [13].

In most of this earlier work, performance under mapping has been assessed as the *variance* of the estimates in relation to the Cramér-Rao bound. General conditions for attaining this bound under mapping were derived by Andersson [3].

In many scenarios however, especially when the bandwidth of a given array is stressed, *mapping bias* can dominate over variance. One example is decade bandwidth signal reconnaissance in the 3-30 MHz band using one single array with a limited number of antennas. In order not to loose resolution such an array has to operate with element spacing in excess of the usual $\lambda/2$ limit at the upper frequencies. Designing the transformation matrix for minimum bias then becomes an issue. -See figure 1.1 for a typical example.

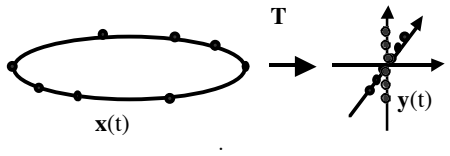

Figure 1.1: A sparse non-uniform circular array, NUCA, whose output vector $\mathbf{x}(t)$ *is mapped by the matrix* $\mathbf{T}$ *onto the output vectors* $\mathbf{y}(t)$ *of a crossed ULA. Two root algorithms, one for each ULA, could then provide fast azimuth as well as elevation estimates. However, the mapping may cause additional stochastic and systematic errors if* $\mathbf{T}$ *is not designed properly.*

II. CONTRIBUTIONS AND REPORT OUTLINE

Usually the transformation matrix $\mathbf{T}$ is designed to provide a least square fit between the spaces spanned by the two sets of response vectors, the real set collected as columns in the matrix $\mathbf{A_r}(\boldsymbol{\theta})$ and the virtual, collected as columns in $\mathbf{A_v}(\boldsymbol{\theta})$. This is done by taking $\mathbf{T} = \mathbf{A_v}(\boldsymbol{\theta})\mathbf{A_r}(\boldsymbol{\theta})^{\dagger}$, where † denotes the Moore-Penrose pseudo-inverse.

In many mapping situations where the least square fit is less than perfect this design of $\mathbf{T}$ is not optimal. The present report proposes an alternative design of $\mathbf{T}$ that greatly can improve the performance of a mapped array by reducing the bias caused by such a mismatch. Simulations show that using the proposed design a mapped circular array like the one in figure 1.1, can operate with up to 4λ element spacing, and still be mapped over a 30^0 wide sector onto a ULA with negligible bias. This would be impossible with the earlier design of $\mathbf{T}$.

Instead of matching the spaces spanned by the two sets of response vectors the alternative design puts the highlight on rotating the mapping errors so that they become orthogonal to the conjugate of the gradient of the estimator cost function along the relevant signal eigenvectors. The design is derived using a Taylor expansion of said cost function

around the true[1] directions of arrival and the corresponding true signal eigenvectors.

The report is organized as follows: After the present introduction the used notation and general assumptions are given. Then the mapping operation is formulated and a Taylor expansion is used to identify the bias mechanism. A general condition for zero bias is then formulated and a design criterion for the transformation matrix given.

Verifying simulations are presented along with a discussion on the problem of simultaneous minimization of both bias and variance. This part couples the proposed mapping method to earlier results by Andersson and Weiss & Friedlander. Finally a two step procedure is suggested that minimizes both bias and variance.

The paper is then concluded with a summation of the findings and a list of references.

III. Data Models and Assumptions

Consider a general planar real array of m_r isotropic antenna elements. The array at this point may be linear, circular or of any arbitrary configuration. Then introduce a spherical coordinate system with azimuth ϕ measured counter-clockwise from the x-axis and elevation θ measured downwards from the z-axis.

Let the incoming signals be described by the d x N vector function **s**[t] where d is the number of signals and $t=t_n$, $1 \le n \le N$ are the time samples (snapshots). We will assume a Gaussian distributed signal model and the usual noise properties of being both temporally and spatially white.

With * denoting Hermitian transpose, the correlation between the d incoming signals is described by the d x d covariance matrix

$$\mathbf{S} = \mathrm{E}\left\{\mathbf{s}(t)\cdot\mathbf{s}^*(t)\right\} \qquad \ldots \quad (3.1)$$

The array output becomes an m_r x N vector function **x**(t)

$$\mathbf{x}(t) = \mathbf{A}_r(\theta)\cdot\mathbf{s}(t) + \mathbf{n}(t) \qquad \ldots \quad (3.2)$$

where the columns[2] of the m_r x d matrix $\mathbf{A}_r(\boldsymbol{\theta})$ transform from the impinging signals **s**(t) to the array output **x**(t), and **n**(t) is the noise contribution from the m_r receiver channels. The p interesting signal parameters (azimuth and elevation) are collected in the parameter matrix $\boldsymbol{\theta}$ of dimension p x d.

To distinguish the real array from the virtual, we will denote the former $\mathbf{A}_r$ as in (3.2) and the latter $\mathbf{A}_v$. The symbols $\hat{\boldsymbol{\theta}}$, $\hat{\phi}$ and $\hat{\theta}$ will be used in the sequel for estimates of the parameter matrix $\boldsymbol{\theta}$, azimuth ϕ and elevation θ respectively.

A. Decomposition into subspaces

For the subspace based DOA estimation methods considered herein, the array output covariance matrix **R** is important:

$$\mathbf{R} = \mathrm{E}\left\{\mathbf{x}(t)\cdot\mathbf{x}^*(t)\right\} = \mathbf{A}(\boldsymbol{\theta})\cdot\mathbf{S}\cdot\mathbf{A}^*(\boldsymbol{\theta}) + \sigma^2\mathbf{I} \qquad \ldots \quad (3.3)$$

It is normally estimated from the array output data by

$$\hat{\mathbf{R}} = \frac{1}{N}\sum_{n=1}^{N}\mathbf{x}(t_n)\cdot\mathbf{x}^*(t_n) \qquad \ldots \quad (3.4)$$

The estimated signal- and noise subspaces of **R**, $\hat{\mathbf{E}}_s$ and $\hat{\mathbf{E}}_n$ respectively, are formed by the eigenvalue decomposition

$$\hat{\mathbf{R}} = \hat{\mathbf{E}}_s\hat{\boldsymbol{\Lambda}}_s\hat{\mathbf{E}}_s^* + \hat{\mathbf{E}}_n\hat{\boldsymbol{\Lambda}}_n\hat{\mathbf{E}}_n^* \qquad \ldots \quad (3.5)$$

B. Problem formulation

Although the underlying application is mapping from a circular array onto a uniform linear array, the argument and derivations will be of a general nature. We will regard the ULA[3] and the associated ULA DOA[4] estimator as one entity, separated from the mapping operation. Hence all estimator cost functions as well as derivatives and gradients thereof will refer to the ULA and its ULA estimator, and be independent of any pre-processing.

The above mentioned mapping errors will be regarded as errors in the (virtual) field that impinges on the ULA and parameterized as corresponding errors $\Delta\mathbf{e}_s$ in the eigen-

[1] The "true" directions may f. ex. be a set of calibrated directions

[2] Often denoted steering- or response vectors. The set of all such vectors within the parameter range of interest will be called the array manifold.

[3] Uniform Linear Array

[4] Direction Of Arrival

vectors $\mathbf{e}_s$ of the signal subspace of the ULA output covariance matrix.

This view will simplify the analysis. The problem of best mapping matrix design can now be formulated as a best transformation on the errors $\Delta\mathbf{e}_s$. We can either minimize them, or rotate them into directions where they cause the least DOA errors, or both.

IV. ARRAY TRANSFORMATIONS

In a practical application it is the output vector $\mathbf{x}_r(t)$ of the real array that is mapped onto the corresponding output vector $\mathbf{x}_v(t)$ of the virtual array, but from (3.2) this is equivalent to performing the same mapping between the two linear spaces spanned by the vectors in the manifolds $\mathbf{A}_r$ and $\mathbf{A}_v$.

The usual, but as we shall see not optimal way, is to design the transformation matrix $\mathbf{T}$ for a least square fit between these two spaces over a certain sector

$$\mathbf{T}^*_{\text{opt}} = \arg\min_{\mathbf{T}^*} \left\| \mathbf{T}^* \cdot \mathbf{A}_r(\boldsymbol{\theta}^{(c)}) - \mathbf{A}_v(\boldsymbol{\theta}^{(c)}) \right\|_F^2 \qquad \ldots \ (4.1)$$

where F denotes the Frobenius norm. The set of directions $\boldsymbol{\theta}^{(c)}$ is normally chosen relatively dense compared to the beamwidth of the real array. If $\mathbf{A}_r$ is not known analytically, $\boldsymbol{\theta}^{(c)}$ can preferably be a set of calibrated directions, hence the superscript $^{(c)}$.

Using the pseudo-inverse $\mathbf{A}^\dagger = \mathbf{A}^*(\mathbf{A}\mathbf{A}^*)^{-1}$ the solution to (4.1) becomes $\mathbf{T}^*_{\text{opt}} = \mathbf{A}_v(\boldsymbol{\theta}^{(c)}) \cdot \mathbf{A}_r(\boldsymbol{\theta}^{(c)})^\dagger$, a matrix that in a least square sense minimizes the mapping errors.

One important prerequisite is that the manifold of the real array does not contain full ambiguities since lack of rank in $\mathbf{A}_r(\boldsymbol{\theta})$ cannot be restored by the transformation. The virtual array can of course always be configured optimally. Since it is virtual it can preferably be a λ/2 spaced ULA at all frequencies and always be oriented perpendicular to the bisector of the chosen calibration sector.

If the minimum in (4.1) is zero, and $\mathbf{T}$ is full rank, the mapping is perfect at the calibrated points $\boldsymbol{\theta}^{(c)}$ and leaves no bias there, and between these (dense) directions the errors will be negligible. However, for mapping between dissimilar or wide spaced arrays over large sectors, perfect match will seldom be the case. In general the mapping will then cause additional DOA estimate bias. If the condition of $\mathbf{T}$ is poor DOA estimate variance increase may also occur. Minimizing the latter comprises the main scope of the present report.

A. *Bias vs. variance*

In many cases bias can dominate over variance. Factors that increase mapping bias are f. ex, dissimilarity between the two arrays, element separation much in excess of λ/2, matching the two arrays over a wide sector, a. s. o.

Figure 4.1 shows such an example. An 8 element 4λ spaced uniform circular array, UCA, is mapped according to (4.1) onto an 8 element λ/2 spaced uniform linear array, ULA, over a 30^0 wide sector. The true DOA is -2^0 and the statistics of 400 root- MUSIC estimates at SNR:s 10, 15, 20, 25, 30, 35 and 40 dB are displayed. The boxes have lines at the lower quartile, median, and upper quartile values. The whiskers show the extent of the rest of the data. Outliers are also marked.

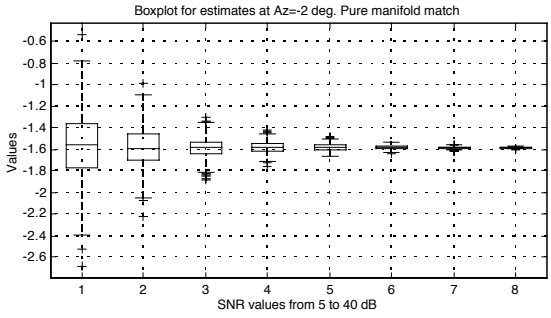

Figure 4.1: The statistics of 400 root MUSIC estimates when an 8 element 4λ spaced UCA is mapped onto an 8 element λ/2 spaced ULA across a 30^0 wide sector. True DOA is -2^0 and bias is evident. The boxes at SNR 10, 15, 20, 25, 30, 35 and 40 dB mark the upper and lower quartile of the DOA estimates. Here bias is the dominating source of error.

To avoid estimator bias caused by coloured noise, the signal subspace was estimated from non-mapped data and thereafter mapped by $\mathbf{T}^*_{\text{opt}}$. The noise subspace needed for MUSIC was then constructed from the corresponding m_r-d smallest singular values. This precaution is necessary because $\mathbf{T}^*_{\text{opt}}$ will in general not be unitary.

In the figure 4.1 case it is clear that for all SNR:s bias dominates over variance. Bias as function of azimuth when the emitter moves across the sector is shown in figure 6.1.

V. A THEORY FOR THE REMOVAL OF MAPPING BIAS

In this section we will derive general principles that govern the magnitude of DOA mapping bias. The result is achieved by giving a geometrical interpretation to the error terms in a Taylor expansion of the DOA estimator cost function. The condition for zero bias is condensed into the orthogonality criterion (5.6) and verified in Section 6 by simulations.

A. The character of mapping bias

It is obvious that in directions where the residual of (4.1) is zero the mapped manifold equals the virtual and no DOA bias *due to the mapping* will occur. This is the case where

$$\Delta\mathbf{A}(\theta) = \mathbf{T}^{*}\mathbf{A}_{r}(\theta) - \mathbf{A}_{v}(\theta) = \mathbf{0} \qquad \ldots \quad (5.1)$$

Due to the deterministic nature of the problem, for given manifolds, DOA estimator and $\mathbf{T}$, the difference $\Delta\mathbf{A}(\boldsymbol{\theta})$ contains enough information to calculate the angular bias that results. In principle the bias therefore can be pre-calculated for each $\boldsymbol{\theta}$ and stored in a look-up table.

A relevant UCA-ULA example is shown in figure 5.1. The arrays have 8 elements separated 2λ and λ/2 respectively.

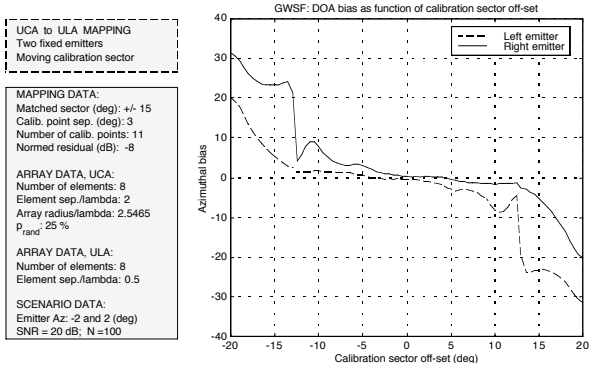

Figure 5.1: UCA-ULA mapping bias when two emitters spaced 10^0 move across and somewhat outside the +/- 15^0 wide mapping sector. As seen bias for both emitters increases sharply as soon as one falls outside the calibrated sector.

A calibration sector of +/- 15^0 is used and $\mathbf{T}$ is calculated according to eq. (4.1) using a 1^0 spaced grid of calibration directions. Each point is based on 100 GWSF[5] runs.

The bias originates in the rather dissimilar array shapes and is magnified by the 2λ element spacing of the UCA. At lower frequencies the bias would be acceptable in many applications, it is the possibility to extend the bandwidth and use wide-spaced array configurations for better resolution that motivates the development of bias removal techniques.

As seen there is also interaction between the two DOA estimates. Compare with figure 6.1 where only one emitter moves across the sector.

B. The gradient with respect to complex vectors

In the analysis below we will need gradients of real scalar functions with respect to complex vectors. We will use the following convention introduced by Brandwood [11]:

Let J($\mathbf{e}$) be a scalar function of the complex vector $\mathbf{e}$ and its conjugate. Furthermore, let $\mathbf{e}_k$ be the k:th component of $\mathbf{e}$ and let x_k and y_k be the real and imaginary part of e_k, respectively. Then the k:th component of the gradient vector is defined as

$$\left[\nabla_{e}\, J(\mathbf{e})\right]_k = \frac{1}{2}\left(\frac{\partial J(\mathbf{e})}{\partial x_k} - j\frac{\partial J(\mathbf{e})}{\partial y_k}\right) \qquad \ldots \quad (5.2)$$

With this convention, the differential of J($\mathbf{e}$) will be $dJ(\mathbf{e}) = 2\,\mathrm{Re}\left\{\left[\nabla_{e}\, J(\mathbf{e})\right]^{T} d\mathbf{e}\right\}$. For the special case of relevance[6] here, J($\mathbf{e}$)=$\mathbf{e}$*$\mathbf{R}$ $\mathbf{e}$, where $\mathbf{R}$ is any Hermitian matrix independent of $\mathbf{e}$, we get $\nabla_{e}\, J(\mathbf{e}) = \mathbf{R}\mathbf{e}$ and $dJ(\mathbf{e}) = 2\,\mathrm{Re}\left\{\mathbf{e}^{T}\mathbf{R}\, d\mathbf{e}\right\}$

C. An analytical description of mapping bias

For all DOA estimators that use a scalar cost function V($\boldsymbol{\theta}$), the maxima or minima of which correspond to the searched directions, the bias situation can be illustrated as in figure 5.2. The variance of the estimates is determined by the curvature ("sharpness") of the cost function, i. e. the slope in the derivative in figure 5.2. This "sharpness" is a feature that is described by the second derivatives and, in zero bias cases, lower bounded by the CRB.

The bias $\Delta\theta$ is described by the off-set in the position of the maximum., or the zero of the (first) derivative in figure 5.2.

[5] Generalized Weighted Subspace Fitting. See Jansson et. al. [10]

[6] Many subspace based DOA estimator cost functions have this structure

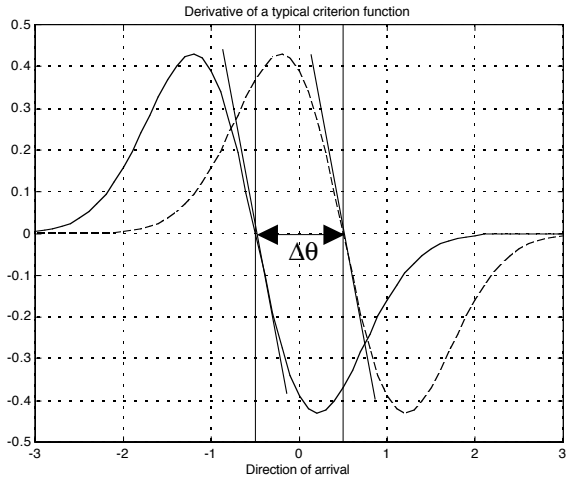

Figure 5.2: A linear approximation of the cost function derivative is sufficient to catch the bias, that is the horizontal displacement $\Delta\theta$.

For a general, enough differentiable cost function $V(\boldsymbol{\theta})$ the maxima or minima occur where the derivatives with respect to the searched parameter θ_i equal zero. Analysing the zeros of the derivatives of $V(\boldsymbol{\theta})$ rather than its extremes is equivalent. This entity will henceforth be denoted $\dot{V}(\boldsymbol{\theta})$ and the corresponding second derivatives $\ddot{V}(\boldsymbol{\theta})$.

In the sequel we will analyse one DOA error at a time, then $\dot{V}(\boldsymbol{\theta})$ and $\ddot{V}(\boldsymbol{\theta})$ are scalars and since they also depend on the (complex) vectors in the signal subspace we will use the notation $\dot{V}(\theta, \mathbf{E}_s)$ and $\ddot{V}(\theta, \mathbf{E}_s)$ respectively.

For scalar DOA errors $\Delta\theta$, a first order Taylor expansion of $\dot{V}(\hat{\theta}, \hat{\mathbf{E}}_s)$ around the true DOA θ and the vectors in the true signal subspace $\mathbf{E}_s$ takes the form, Brandwood [11],

$$\dot{V}(\hat{\theta}, \hat{\mathbf{E}}_s) = \dot{V}(\theta, \mathbf{E}_s) + \ddot{V}(\theta, \mathbf{E}_s) \cdot \Delta\theta + \ldots$$
$$\ldots + 2\sum_{i=1}^{d} \mathrm{Re}\left\{ (\nabla_{\mathbf{e}_i} \dot{V}(\theta, \mathbf{E}_s))^T \Delta \mathbf{e}_i \right\} + \mathrm{rem} \qquad \ldots \quad (5.3)$$

where $\nabla_{\mathbf{e}_i}$ is the complex gradient along vector $\mathbf{e}_i$ in the signal subspace $\mathbf{E}_s$. and $\Delta\mathbf{e}_i$ are the signal eigenvector mapping errors. The remainder term 'rem' is at least quadratic in $\Delta\theta$ and $\Delta\mathbf{E}_s$ and can be neglected if $\dot{V}(\boldsymbol{\theta})$ behaves "well" and the amount of bias $\Delta\theta$ is limited.

We now observe that $\hat{\theta}$ and $\hat{\mathbf{E}}_s$ are estimated at the extremes of the cost function, i. e. where the scalar entities $\dot{V}(\hat{\theta}, \hat{\mathbf{E}}_s)$ and $\dot{V}(\theta, \mathbf{E}_s)$ both equal zero. Hence, using (5.3) we can express the modulus of the bias $\Delta\theta$ as

$$|\Delta\theta| \le \left| \left[\ddot{V}(\theta, \mathbf{E}_s) \right]^{-1} \right| \cdot \left| 2\sum_{i=1}^{d} \mathrm{Re}\left\{ (\nabla_{\mathbf{e}_i} \dot{V}(\theta, \mathbf{E}_s))^T \Delta \mathbf{e}_i \right\} \right| \qquad (5.4)$$

an entity that we want to minimise. The leading Hessian inverse is difficult to manipulate but the second term with the gradients and the signal eigenvector mapping errors offers a possibility that now will be exploited.

Inside the Re operator each term can be interpreted as the inner product between the conjugate of the gradient of $\dot{V}$ along the i:th signal eigenvector, and the mapping error in that particular signal eigenvector. This geometrical interpretation will now be used to form a criterion that errors of all kinds must fulfil in order not to result in systematic DOA errors, i. e. bias.

C. A criterion for zero mapping bias

In view of the structure of (5.4) we conclude that a *sufficient condition for zero bias* is

$$\bar{\mathbf{g}}^{(i)} \perp \Delta \mathbf{e}_i, \quad i \in \{1, .., d\} \qquad \ldots \quad (5.5)$$

where $\bar{\mathbf{g}}^{(i)} \stackrel{\Delta}{=} \overline{\nabla_{\mathbf{e}_i} \dot{V}_{MU}(\theta, \mathbf{E}_s)}$.

This means that in a given mapping scenario, for each signal eigenvector of $\mathbf{R}$ the mapping matrix $\mathbf{T}$ should have the property to leave signal eigenvector mapping errors that are orthogonal to the conjugate of the gradient of the cost function $\dot{V}$ in that particular signal eigenvector direction. Where this is the case, the mapping errors do not effect the cost function and hence do not cause bias. This holds for all errors $\Delta\mathbf{e}_i$ that are small enough for the Taylor expansion (5.3) to be valid.

For a full rank signal covariance matrix and high SNR, at each true DOA we have for the two ranges $\Re$:

$$\Re\left\{ \mathbf{T}^* \mathbf{A}_r \right\} = \Re\left\{ \hat{\mathbf{E}}_s \right\} \qquad \ldots \quad (5.6)$$

and likewise for the virtual array $\Re\{\mathbf{A}_v\} = \Re\{\mathbf{E}_s\}$. In addition, at each true (bias free) DOA $\bar{\mathbf{g}}^{(i)} \perp \mathbf{E}_s^{(i)}$. Hence, if we design $\mathbf{T}$ so that $\Re\left\{ \mathbf{T}^* \mathbf{A}_r^{(i)} \right\} = \Re\left\{ \mathbf{A}_v^{(i)} \right\}$, the mapping error $\Delta\mathbf{A}(\theta^{(i)})$ can be used in stead of $\Delta\mathbf{e}_i$ in (5.5). This is because the error vectors $\Delta\mathbf{A}(\theta^{(i)})$ and $\Delta\mathbf{e}_i$ then become parallel.

We can now reformulate the condition (5.5) into the following more useful requirement:

$$\Delta\mathbf{A}(\theta^{(i)}) \perp \bar{\mathbf{g}}^{(i)}, \quad \forall i = 1,\ldots,N_{cal} \qquad \ldots \quad (5.7)$$

Generally if $\Delta\mathbf{A}\neq\mathbf{0}$, by maintaining the orthogonalities (5.7) in some directions, bias can be made arbitrarily small in those directions.

Condition (5.7) holds for all types of errors, not only mapping errors. It will now be used across large sectors where $N_{cal} > m_r$ and a least square compromise for $\mathbf{T}$ has to be found. This case is of interest in signal surveillance such as the SESAM application where the DOAs initially are completely unknown and we need to combine omni-dirctionality (the circular real array) with processing speed (the ULA based root estimators).

*D. A design of **T** for minimum bias*

At each of the N_{cal} calibration directions in the sector the response vector matrix mapping error is

$$\Delta\mathbf{A}(\boldsymbol{\theta}^{(i)}) = \mathbf{T}^*_{opt}\mathbf{A}_r(\boldsymbol{\theta}^{(i)}) - \mathbf{A}_v(\boldsymbol{\theta}^{(i)}) \qquad \ldots \quad (5.8)$$

where i=1,..., N_{cal}. Since bias is created by the part of $\Delta\mathbf{A}(\boldsymbol{\theta}^{(i)})$ that falls within $\Re\{\bar{\mathbf{g}}(\theta)\}$ an optimal transformation matrix $\mathbf{T}$ should minimize the real part of all N_{cal} scalar products $\bar{\mathbf{g}}(\theta^{(i)})\cdot\Delta\mathbf{A}(\boldsymbol{\theta}^{(i)})$ across the sector.

Taking this into account and introducing the weighting constant k, $0\le k\le 1$, the following cost function for the design of $\mathbf{T}$ is proposed

$$\mathbf{T}^*_{opt} = \arg\min_{k,\mathbf{T}^*}\Big\{(1-k)\big\|\mathbf{T}^*\cdot\mathbf{A}_r(\theta) - \mathbf{A}_v(\theta)\big\|_F^2 + \ldots + k\cdot\sum_{i=1}^{N_{cal}}\Big\|\mathrm{Re}\big\{\mathbf{g}^{(i)T}\cdot\mathbf{T}^*\mathbf{A}_r(\theta^{(i)}) - \mathbf{g}^{(i)T}\mathbf{A}_v(\theta^{(i)})\big\}\Big\|_F^2\Big\} \qquad (5.9)$$

It consists of the original manifold matching expression in (4.1) plus one penalty term for each calibration direction. The latter terms penalize non-orthogonalities in (5.6) to an amount proportional to k.

At this point the weighting constant k is unknown. Its optimum value depends on the two array manifolds, the SNR and other parameters in the scenario. Initially it therefore has to be chosen empirically, see figure 6.3.

The minimization problem (5.9) can be solved in many ways. One approach is to apply the vec operator to both terms inside each Frobenius norm and solve for a vectorized version $\mathbf{t}$ of $\mathbf{T}^*_{opt}$. Then we first reverse order between terms in (5.9) by taking Hermitian transpose

$$\mathbf{T}^*_{opt} = \arg\min_{\mathbf{T}^*}\Big\{(1-k)\big\|\mathbf{A}_r^*(\theta)\cdot\mathbf{T}\cdot\mathbf{I} - \mathbf{A}_v^*(\theta)\big\|_F^2 + k\cdot\sum_{i=1}^{N_{cal}}\Big|\mathrm{Re}\big\{\mathbf{A}_r^*(\theta^{(i)})\cdot\mathbf{T}\cdot\bar{\mathbf{g}}^{(i)} - \mathbf{A}_v^*(\theta^{(i)})\bar{\mathbf{g}}^{(i)}\big\}\Big|^2\Big\} \qquad (5.10)$$

and thereafter apply the vec operator to get

$$\mathbf{T}^*_{opt} = \arg\min_{\mathbf{T}^*}\Big\{(1-k)\big\|\mathbf{I}\otimes\mathbf{A}_r^*(\theta)\,\mathrm{vec}(\mathbf{T}) - \mathrm{vec}(\mathbf{A}_v^*(\theta))\big\|_F^2 + k\cdot\sum_{i=1}^{N_{cal}}\Big|\mathrm{Re}\big\{\mathbf{g}^{(i)*}\otimes\mathbf{A}_r^*(\theta^{(i)})\,\mathrm{vec}(\mathbf{T}) - \mathrm{vec}(\mathbf{A}_v^*(\theta^{(i)})\bar{\mathbf{g}}^{(i)})\big\}\Big|^2\Big\} \qquad \ldots \quad (5.11)$$

In (5.11) we have used that for any matrices $\mathbf{A}$, $\mathbf{B}$ and $\mathbf{C}$,

$$\mathrm{vec}(\mathbf{ABC}) = \mathbf{C}^T\otimes\mathbf{A}\;\mathrm{vec}(\mathbf{B}) \qquad \ldots \quad (5.12)$$

where $\otimes$ is the Kronecker product. The first norm in (5.9) contains a term of dimension $m_v N_{cal}$ x 1, whereas all the penalty terms have dimension m_v x 1.

Introducing the short hand notation

$$\mathbf{M}_1 = \sqrt{1-k}\cdot\mathbf{I}\otimes\mathbf{A}_r^*(\theta) \qquad \ldots \quad (5.13)$$

of size $m_v N_{cal}$ x $m_v\, m_r$,

$$\mathbf{m}_2 = \sqrt{1-k}\cdot\mathrm{vec}(\mathbf{A}_v^*(\theta)) \qquad \ldots \quad (5.14)$$

of size $m_v N_{cal}$ x 1,

$$\mathbf{M}_3^{(i)} = \sqrt{k}\cdot\mathbf{g}^{(i)*}\otimes\mathbf{A}_r^*(\theta^{(i)}) \qquad \ldots \quad (5.15)$$

of size 1 x $m_v\, m_r$, and finally

$$\mathbf{m}_4^{(i)} = \sqrt{k}\cdot\mathrm{vec}(\mathbf{A}_v^*(\theta^{(i)})\bar{\mathbf{g}}^{(i)}) \qquad \ldots \quad (5.16)$$

of size 1 x 1, we get from (5.11) by stacking terms

$$\mathbf{T}^*_{\text{opt}} = \arg\min_{\mathbf{T}^*} \left\| \begin{bmatrix} \text{Re}\{\mathbf{M}_1\} & -\text{Im}\{\mathbf{M}_1\} \\ \text{Im}\{\mathbf{M}_1\} & \text{Re}\{\mathbf{M}_1\} \\ \text{Re}\{\mathbf{M}_3^{(1)}\} & -\text{Im}\{\mathbf{M}_3^{(1)}\} \\ \vdots & \vdots \\ \text{Re}\{\mathbf{M}_3^{(N_{cal})}\} & -\text{Im}\{\mathbf{M}_3^{(N_{cal})}\} \end{bmatrix} \cdot \begin{bmatrix} \text{vec}(\text{Re}\{\mathbf{T}\}) \\ \text{vec}(\text{Im}\{\mathbf{T}\}) \end{bmatrix} - \begin{bmatrix} \text{Re}\{\mathbf{m}_2\} \\ \text{Im}\{\mathbf{m}_2\} \\ \mathbf{m}_4^{(1)} \\ \vdots \\ \mathbf{m}_4^{(N_{cal})} \end{bmatrix} \right\| \quad (5.17)$$

Using the further short hand notation

$$\mathbf{T}^*_{\text{opt}} = \arg\min_{\mathbf{T}^*} |\mathbf{M}\cdot\mathbf{t} - \mathbf{m}|^2 \quad \ldots \quad (5.18)$$

for (5.17), with obvious definitions for **M**, **t** and **m**, the searched transformation matrix is obtained from the least square solution

$$\mathbf{t} = \begin{bmatrix} \text{vec}(\text{Re}\{\mathbf{T}\}) \\ \text{vec}(\text{Im}\{\mathbf{T}\}) \end{bmatrix} = \mathbf{M}^{\dagger}\cdot\mathbf{m} \quad \ldots \quad (5.19)$$

It involves calculating the Moore-Penrose pseudoinverse of a large (full rank) matrix of size $(2m_v+1)N_{cal}$ x $2m_v m_r$. If, as a typical example, $m_v=m_r=8$ and $N_{cal}=15$, the size of the matrix is 255 x 128.

This size will not slow down real time operation of a DF[7] system however, since all mapping matrices, one for each sector, can be calculated in advance in conjunction with a calibration process.

Note that in the above derivation of the expression (5.10) no restrictions on the cost function V were made other than the existence of the necessary derivatives. Hence we conclude (5.10) to be applicable for all DOA estimators that are based on cost functions of this class.

Also note that if the virtual array in combination with the used DOA estimator is exactly bias free, then $\mathbf{A}_v^*(\theta^{(i)})\bar{\mathbf{g}}^{(i)} = 0, \forall i$ and (5.10) can be somewhat simplified. Since this is the usual case[8] we see that we cannot allow k=1 for then **T**=**0** would be an obvious, but not wanted, solution to (5.10).

Finally, if the antenna elements are modeled through their phase lags only and k is close to 1, then the degrees of freedom in the two spaces that $\mathbf{T}^*_{\text{opt}}$ shall match are few. Simulations show that in such cases we can drop the Re operator in (5.10). This appreciably reduces the size of the equation system that solves (5.9) and may therefore be preferable.

Despite the fact that we now require **T** to minimize *both* the real and imaginary parts of the scalar products $\mathbf{g}^{(i)T}\cdot\mathbf{T}^*\mathbf{A}_r(\theta^{(i)})$, a sufficiently good solution will be found anyway. This will also robustify the propsed algorithm in that it becomes insensitive to unintentional rotation of the (complex) numbers $\mathbf{g}^{(i)T}\cdot\mathbf{T}^*\mathbf{A}_r(\theta^{(i)})$ in the complex plane.

Such unintentional rotations can be caused by f. ex. the omitted rest terms in the Taylor expansion (5.2). These rest terms become important when the linear term is reduced imposing the orthogonality criterion (5.5).

E. The weighting constant k

The scalar product between the manifold mapping error $\Delta\mathbf{A}$ and the gradient $\bar{\mathbf{g}}$, a product the real part of which we want to minimize, can be made small via two mechanisms:

(i) Orthogonality between the two involved vectors

(ii) Small length for at least one involved vector

The sum term in (5.10) secures (i) and the manifold matching term (ii). The weighting constant k thus provides a possibility to find a suitable mix between (i) and (ii).

To illustrate the problem of picking the optimal k we consider the calibration process (which is carried out against one emitter at a time). Then both the gradient $\bar{\mathbf{g}}$ and the mapping error $\Delta\mathbf{A}$ are m_r x 1 vectors, see figure 5.3 for a 2D illustration.

From figure 5.3 we conclude that using a k-value near 1, which puts less emphasis on minimizing the length of the manifold mapping error $\Delta\mathbf{A}$, requires good accuracy in the orthogonality if bias is to be kept down.

[7] Direction Finding

[8] This generally presumes that finite sampling effects are negligible, see Xu & Buckley [2] for reference.

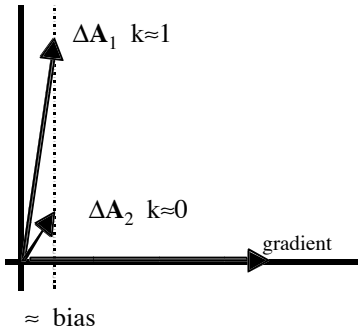

Figure 5.3: For a given acceptable bias (scalar product between $\bar{g}$, and $\Delta\boldsymbol{A}$), the larger the k, the less control over the size of the mapping error $\Delta\boldsymbol{A}$ but the more perfect an orthogonality we enforce. Above $\Delta\boldsymbol{A}_1$ corresponds to a large k and $\Delta\boldsymbol{A}_2$ to a small one.

As a consequence, the higher k-value we want to use, the better SNR we need. For the extreme case where k=1, i. e. all requirements on manifold match are dropped, we can expect running into numerical problems, especially if a bias-free DOA estimator is used so that |**T**] approaches zero. On the other extreme, i. e. k=0, we can only achieve zero bias where the manifold mapping is perfect, $\Delta\mathbf{A}$=0. For dissimilar arrays this generally requires the DOA to be known.

If the two arrays are dissimilar, f. ex. UCA-ULA mapping and we want to design a **T** for a finite sector, both extremes will be sub-optimal and the best k is somewhere in between. See figure 6.3 for an illustrative example.

VI. Verifying Simulations

A. Root-MUSIC and UCA-ULA mapping

In the usual MUSIC power spectrum

$$P_{MU} = \frac{\mathbf{a}^*(\boldsymbol{\theta})\mathbf{a}(\boldsymbol{\theta})}{\mathbf{a}^*(\boldsymbol{\theta})\mathbf{E}_n\mathbf{E}_n^*\mathbf{a}(\boldsymbol{\theta})} \quad \ldots (6.1)$$

the null spectrum in the denominator

$$V_{MU}(\boldsymbol{\theta},\hat{\mathbf{E}}_S) \triangleq \ldots = \mathbf{a}^*(\boldsymbol{\theta})\mathbf{E}_n\mathbf{E}_n^*\mathbf{a}(\boldsymbol{\theta}) = \mathbf{a}^*(\boldsymbol{\theta})(\mathbf{I}-\mathbf{E}_S\mathbf{E}_S^*)\mathbf{a}(\boldsymbol{\theta}) \quad \ldots (6.2)$$

can be used as the cost function. We can equivalently study the off-set in the zeros of its derivative, see (5.3),

and therefore form the new cost function, Brandwood [11]

$$\dot{V}_{MU}(\theta,\hat{\mathbf{E}}_S) \triangleq \frac{\partial V_{MU}(\theta,\hat{\mathbf{E}}_S)}{\partial\theta} = 2\,\mathrm{Re}\left\{\mathbf{a}^*(\theta)(\mathbf{I}-\mathbf{E}_S\mathbf{E}_S^*)\dot{\mathbf{a}}(\theta)\right\} \quad \ldots (6.3)$$

The derivative in the second term of the Taylor expansion (5.4) becomes

$$\ddot{V}_{MU}(\theta,\mathbf{E}_S) = 2\dot{\mathbf{a}}^*(\theta)\cdot(\mathbf{I}-\mathbf{E}_S\mathbf{E}_S^*)\cdot\dot{\mathbf{a}}(\theta) \quad \ldots (6.4)$$

where $\dot{\mathbf{a}}^*$ denotes the Hermitian transpose of the derivative of $\mathbf{a}$ with respect to θ. Furthermore the gradient of $\dot{V}_{MU}(\theta,\mathbf{E}_S)$ with respect to the eigenvector $\mathbf{e}_i$ becomes

$$\nabla_{\mathbf{e}_i}\dot{V}_{MU}(\theta,\mathbf{E}_S) = -\overline{\dot{\mathbf{a}}}(\theta)\mathbf{e}_i^*\,\mathbf{a}(\theta) - \overline{\mathbf{a}}(\theta)\mathbf{e}_i^*\,\dot{\mathbf{a}}(\theta) \quad \ldots (6.5)$$

Hence, for MUSIC the zero bias condition (5.8) is the real part of the orthogonality relation

$$\bar{\mathbf{g}}^{(i)} \triangleq \overline{\nabla_{\mathbf{e}_i}\dot{V}_{MU}(\theta,\mathbf{E}_S)} = \overline{\dot{\mathbf{a}}(\theta^{(i)})\mathbf{e}_i^*\,\mathbf{a}(\theta^{(i)}) + \overline{\mathbf{a}}(\theta^{(i)})\mathbf{e}_i^*\,\dot{\mathbf{a}}(\theta^{(i)})} \perp \Delta\mathbf{e}_i, \quad i\in(1,N_{cal}) \quad \ldots (6.6)$$

In the simulations to follow a single emitter that sweeps a 30^0 wide calibration sector was used. The sector has 15 equispaced calibrated directions and it is assumed that calibration is performed against one emitter at a time. The 15 calibration response vectors are used in the calculation of **T** according to (5.10), and, for reference, also (4.1).

The number of snapshots was 100 and SNR per array element rather high to highlight mapping effects. Bias values are generated as the difference between the true directions and estimates from the mapped data. Each such estimate uses 400 standard root-MUSIC Monte Carlo runs.

In figures 6.1-6.2 the real array is an 8 element UCA spaced at 4λ i. e. well in excess of the usual λ/2 limit. It thus possesses slight, but due to the circular shape, not full ambiguities and is therefore also more prone to generating bias. The virtual array is an 8 element ULA spaced at λ/2 and oriented perpendicular to the bisector of the calibration sector.

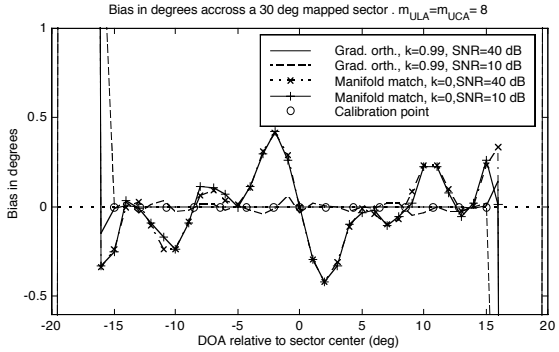

Figure 6.1: At k=0.99 maximum bias is reduced 50-100 times by the proposed design of the transformation matrix as compared to the pure manifold matching design. See fig. 6.2 for a magnified version.

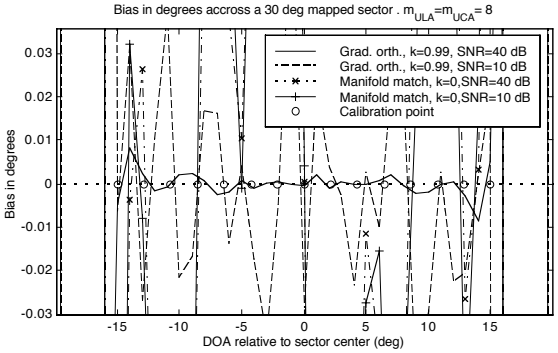

Figure 6.2. The scenario as in figure 6.1 but magnified to highlight the small bias that results from the proposed algorithm (5.9). The bias reduction is ueful even at SNR = 10 dB.

B. The weighting constant k

Influence on the mapping bias of the weighting constant k is illustrated in figure 6.3 for 8 to 8 element UCA-ULA mapping. The UCA is spaced 4λ and the ULA λ/2. The figure shows the r.m.s. of all the bias values inside the calibration sector for 0≤k≤1 with the parameter values SNR 10 and 40 dB.

Again it is seen that only at the highest SNR is it possible to stress the orthogonality condition (5.6) to the extreme by picking a k near 1. However, if we refrain from this the value of k is not critical. This shows a certain amount of robustness for the proposed bias reduction mapping algorithm.

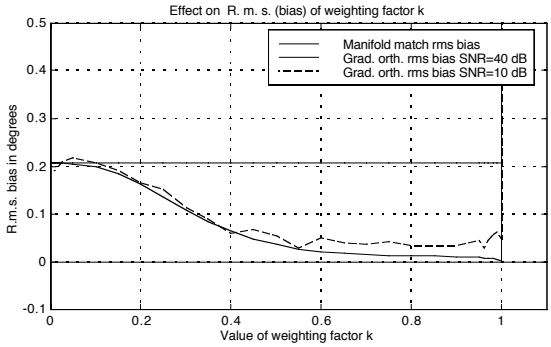

Figure 6.3: R.m.s. of the all the mapped DOA bias values inside a 30^0 wide sector as function of the weighting constant k with SNR as parameter. The reference line corresponds to pure manifold match, i. e. k=0.

VII. MINIMIZING BOTH BIAS AND VARIANCE

The total mean square DOA errors (mse) consists of both bias and variance so a natural boundary condition on any bias reduction method is that it must not increase variance to an extent where the total mse increases.

Andersson [3] has given the following two conditions for the DOA estimate variance to attain its Cramér-Rao Bound, CRB, under mapping

$$\mathbf{\Pi}_{\mathbf{T}_{\text{opt}}^*}\,\mathbf{A}(\boldsymbol{\theta}_0)=\mathbf{A}(\boldsymbol{\theta}_0) \qquad \ldots \quad (7.1)$$

$$\mathbf{\Pi}_{\mathbf{T}_{\text{opt}}^*}\,\mathbf{\Pi}_{\mathbf{A}_r}^{\perp}\,\mathbf{D}(\boldsymbol{\theta}_0)=\mathbf{\Pi}_{\mathbf{A}_r}^{\perp}\,\mathbf{D}_r(\boldsymbol{\theta}_0) \qquad \ldots \quad (7.2)$$

where the response vector derivatives

$$\mathbf{D}=\left[\left.\frac{\partial\mathbf{a}(\theta)}{\partial\theta}\right|_{\theta=\theta_0^{(1)}},\ldots,\left.\frac{\partial\mathbf{a}(\theta)}{\partial\theta}\right|_{\theta=\theta_0^{(N_{cal})}}\right] \qquad \ldots \quad (7.3)$$

In (7.1) and (7.2) the projector on the range space of $\mathbf{T}_{\mathbf{opt}}$ is $\Pi_{\mathbf{T}_{\text{opt}}^*}=\mathbf{T}_{\text{opt}}(\mathbf{T}_{\text{opt}}^*\mathbf{T}_{\text{opt}})^{-1}\mathbf{T}_{\text{opt}}^*$ and the above condition essentially says that the mapping matrix $\mathbf{T}$ must retain all the dimensions needed for $\mathbf{A}_r$ and its derivatives $\mathbf{D}$. Otherwise the Cramér-Rao limit for the unmapped DOA estimate variance will not be attained.

A. The condition of the mapping matrix

A general problem with sector mapping is the condition of the mapping matrix. The response vectors from the different calibration directions will often get linearly dependent, see figure 7.1

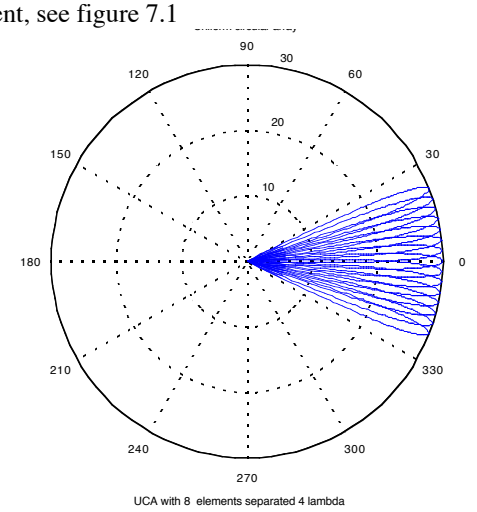

Figure 7.1.With 4 wavelengths of UCA element separation a 45^o sector can barely encompass m linearly independent response vectors. m is the number of antenna elements.

If these vectors are used to calculate the mapping matrix, said matrix will be of poor condition and the estimated DOAs will suffer added variance. With 4 wavelengths of UCA element separation a 45 deg sector can barely encompass m linear independent response vectors. m is the number of antenna elements.

The maximum number N_{rv} of (sufficiently) independent response vectors inside a certain sector of width S_w can be approximated by S_w/B_w where B_w is the array beamwidth. To solve the equation system (5.18) we should have $N_{rv} \geq m$, were m is the number of array elements. Strict inequality is to prefer since it leads to a numerically more robust least square solution for the best mapping matrix.

Taking a uniform $\lambda/2$ spaced circular array UCA as an example we roughly have

$$B_w = \lambda / (m \frac{\lambda}{2} \frac{1}{\pi}) = \frac{2\pi}{m} \quad \ldots \quad (7.4)$$

The above unequality $N_{rv} \geq m$ then becomes

$$N_{rv} = S_w / B_w = S_w / (\frac{2\pi}{m}) \geq m \quad \ldots \quad (7.5)$$

which yields $S_w \geq 2\pi \quad (\forall m\,!)$. Since this is impossibly wide for a good circular to linear match we must increase the element spacing. In Hyberg [1] it is shown that up to 4λ is quite feasible for an UCA, and this would yield $B_w = \pi/(4m)$ and $S_w \geq \pi/4$ respectively.

This situation is plotted in figure 7.1 and is numerically much easier to handle. As a compromise between linear dependence and mapping errors a sector width of 30^0 can be used.

Hence we see that sector mapping always has to be performed with some linear dependence among the used calibration steering vectors. This leads to increased variance and is a general drawback for the UCA-ULA mapping approach.

The above problem motivates the development of techniques to reduce this extra variance while at the same time keeping bias small. This will be the scope of a future companion report.

B. A multi-step procedure

If the array manifold matrix $\mathbf{A}_r$ is ill conditioned the calculated $\mathbf{T}$ will also get ill conditioned since this calculation is based on $\mathbf{A}_r$. This means that some of the m dimensions are poorly spanned and the CRB retainment condition (7.1) & (7.2) will not be fully met.

We can use dimension reduction and remove those directions (eigenvectors) of $\mathbf{T}$ that correspond to the smallest singular values, in order to improve the condition, but this in principle requires knowledge of the true DOA. Since the DOA is unknown we therefore have to use a multi-step procedure involving successive sector width- and dimension reduction ($m_v < m_r$):

(i) Use a calibrated sector, f. ex. 30^0 wide and algorithm (5.8) to get the preliminary DOAs. Select one of these

(ii) Shrink the sector around this DOA down to a fraction of the beamwidth

(iii) Reduce the number of elements in the virtual array until $\mathbf{T}_{opt}^{*}\mathbf{T}_{opt}$ constructed through (5.8) becomes full rank.

(iv) Perform the mapping

(v) Use any efficient algorithm to estimate the DOA from the mapped data

Step (iii) means projecting away those dimensions in the space spanned by $\mathbf{T}_{opt}^{*}\mathbf{T}_{opt}$ that correspond to the smallest singular values, Andersson [3]. Thus the main dimensions are retained and the requirements (7.1) and (7.2) met as well as possible.

VIII. CONCLUSIONS

Antenna array mapping is a powerful tool in that it allows fast DOA estimation algorithms usually requiring ULAs to be used on any array shape. One attractive application is signal reconnaissance where the need for omni-directionality requires a circular array and the simultaneous need for processing speed requires a linear. Finding an optimal mapping procedure therefore is of great interest.

This work has shown that when mapping the output data vector from one (real) array onto the output data vector of another (virtual) array, the usual least square fitting of the spaces spanned by the two sets of response vectors, is not optimal. Apart from increased variance, bias will occur, a bias that can dominate over variance, especially in broad band applications when element spacing can be large compared to $\lambda/2$. It was also shown that such wide element spacing is needed to avoid linear dependence among the response vectors comprising a mapped sector.

It was found that this bias can be substantially reduced by adding a sequence of penalty terms to the usual manifold matching criterion. The decisive key property of the improved criterion is that it takes orthogonality between the gradients of the estimator cost function and the mapping errors into account. A bias reduction factor of up to 100 or more has been demonstrated in this report.

The role of these orthogonalities was unveiled using a Taylor expansion of a general DOA estimation cost function. Their importance is illustrated by a rather high weighting factor for the penalty terms in an optimally designed cost function for the transformation matrix.

The exact values of the optimal weighting factor k was found not to be critical, indicating a robustness of the proposed method. However, using a k near 1 requires a rather high SNR.

REFERENCES

[1] B. Friedlander, "Direction Finding Using Spatial Smoothing With Interpolated Arrays", IEEE Transactions on Aerospace and Electronic Systems", April 1992.

[2] X-L Xu, K. M. Buckley, "Bias Analysis of the MUSIC Location Estimator", IEEE Transactions on Signal Processing, vol. 40, N:o 10, October 1992

[3] S. Andersson: , "On Dimension Reduction in Sensor Array Processing", PhD Thesis, Linköping University, 1992.

[4] B. Friedlander, "The Root-MUSIC Algorithm for Direction Finding with Interpolated Arrays", Signal Processing 30, 1993, pp. 15-29

[5] A. J. Weiss, B. Friedlander, "Performance Analysis of Spatial Smoothing with Interpolated Arrays", IEEE Transactions on Signal Processing, May 1993

[6] A. J. Weiss, B. Friedlander, "Preprocessing for Direction Finding with Minimal Variance Degradation", IEEE Transactions on Signal Processing, June 1994

[7] A. Weiss, B. Friedlander, P. Stoica, "Direction of Arrival Estimation Using MODE with Interpolated Arrays", IEEE Transactions of Signal Processing, January 1995

[8] J. Eriksson, M. Viberg, "Data Reduction in Spatially Colored Noise using a Virtual Uniform Linear Array", Proceedings of ICASSP 2000.

[9] Per Hyberg, " Circular to Linear Array Mapping using Calibration Data". IEE Eighth International Conference on HF Radio Systems and Techniques, July 2000, pp. 71-75

[10] M. Jansson, A. Lee Swindlehurst, B. Ottersten, ”Weighted Subspace Fitting for General Array Models”, IEEE Trans. on Signal Processing, vol 46, No 9, Sept 1998.

[11] D. H. Brandwood, “A complex gradient operator and its application in adaptive array theory”, Proc. Inst. Electr. Eng., vol 130, parts F and H, no. 1, pp. 11-16, Feb. 1983.

[12] P. Hyberg, "Circular to Linear Array Mapping and Bias Reduction", Lic. thesis, ISSN 1103-8039, ISRN KTH/SB/R--01/19--SE, September 2001.

[13] J. Eriksson, "On detection and Estimation of Multiple Sources in Radar Array Processing", Dr thesis, CTH 2002. Series 1793, ISSN 0346-718X

[14] P Hyberg, M. Jansson, B Ottersten, "Array Mapping Optimal Transformation Matrix Design". In proceedings of ICASSP 2002.